Effect of Active Species Mobility on Soot-Combustion over Cs-V Catalysts

Debora Fino, Nunzio Russo, Claudio Badini, Guido Saracco, and Vito Specchia
Dipt. di Scienza dei Materiali ed Ingegneria Chimica, Politecnico di Torino, Corso Duca degli Abruzzi 24, 10129 Torino, Italy

The soot combustion process promoted by some of the most promising diesel particulate combustion catalysts ($Cs_2O \cdot V_2O_5$, $Cs_4V_2O_7$, $CsVO_3$) is discussed on the grounds of a theoretical analysis and an experimental test campaign involving reaction runs in microreactors (either in isothermal or in temperature-programmed conditions) and in a DSC apparatus. Such investigations, beyond the prevalent kinetic parameters (activation energy, oxygen reaction order, preexponential kinetic constant), led to a definition of the role of catalyst-to-carbon contact conditions on the conversion rate. Particularly, the role of formation of eutectic liquid phases, which dominates the catalytic behavior of the $Cs_2O \cdot V_2O_5$ catalyst, was fully elucidated on the grounds of either DSC runs or visual inspection through a heated optical microscope.

Introduction

The emissions of diesel engines are harmful for both human health and the environment, especially because of their high content of particulate and nitrogen oxides. Owing to its small size, diesel particulate can be retained in the alveolar region of the lungs where it can promote cancer. Hence, the increase in the diesel-vehicles market has brought many countries, such as the U.S., Japan, and Europe, to introduce specific limits to exhaust-gas emissions. Quite severe limits have been fixed for the year 2005 (0.025 g/km). This will require significant progress in the R&D of specific after-treatment devices (Konstandopoulos et al., 2000). In this context, our group is working as a partner of industrial-type European projects (such as CATATRAP, ART-DEXA, and SYLOC-DEXA) that involve, as well, several partners from the automotive, catalyst, and trap manufacturing industries in the development of ad hoc–designed catalytic traps. The catalyst deposited in such devices should lower the soot ignition temperature (about 600°C for noncatalytic combustion) down to the values characteristic of diesel exhaust gases (180–350°C) so as to enable self-regeneration of the traps. Earlier studies carried out at Politecnico di Torino concerned the development of soot combustion catalysts based on Cs and V oxides for catalytic foam traps (Saracco et al., 1999; Badini et al., 2000). The aim of the work is to analyze the soot combustion process promoted by these catalysts, also on the grounds of kinetics assessment experiments, paying particular attention to the role of mobile catalyst species on the reaction process.

Correspondence concerning this article should be addressed to D. Fino.

Challenges and Pitfalls

Diesel particulate

Diesel particulate is composed of carbon particles of the average formula C_8H on which hydrocarbons are adsorbed. More precisely, it consists of soot nuclei (carbon), adsorbed hydrocarbons [often referred to as soluble organic fraction (SOF), which includes PAH and nitro-PAH], sulphates, water, and trace amounts of zinc, phosphorus, calcium, iron, silicon, and chromium (Neeft et al., 1996). The noncatalytic ignition temperature of soot depends on the content of adsorbed hydrocarbons, but generally exceeds 600°C. Moreover, the composition of diesel particulate is affected by several engine operation characteristics such as load, speed, and operating temperatures, as the amount of SOF highly depends on cylinder temperature. Thus, it is difficult to collect batches of soot with constant properties. As a consequence, real soot is substituted in numerous investigations by several carbonaceous structures such as carbon blacks (Liu et al., 2001), amorphous carbon (Serra et al., 1997), and industrial-model soot (Mul et al., 1995).

Catalyst

Several catalysts were proposed and tested according to the literature: precious metals (Pt, Pd and Rd; Mariangeli et al., 1987); metal oxides (of alkali metals, copper, vanadium, molybdenum, etc.; Ahlstrom and Odenbrand, 1990; McKee and Chatterji, 1975); Cu-K-V-Cl and Cu-K-Mo-Cl systems capable of providing mobile catalytic species (vapor or liquid)

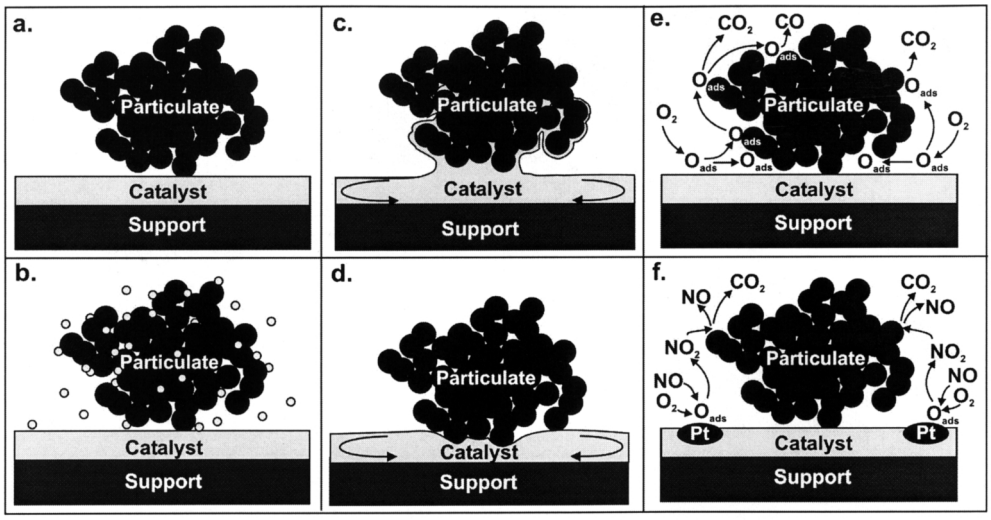

Figure 1. Alternatives for coupling catalysts and traps for trap regeneration purposes.

Legend: (a) nonmobile catalyst; (b) gas-phase mobile catalyst; (c) wetting mobile catalyst; (d) nonwetting mobile catalyst; (e) catalyst promoting oxygen spillover; (f) catalyst coupling a NO/NO_2 functionality (indirect catalyst).

that enhance the soot-catalyst contact area (Watabe et al., 1983; Ciambelli et al., 1996; Mul et al., 1995; Serra et al., 1997; Saracco et al., 1997); other mobile catalysts based on alkali vanadates (Badini et al., 2000). Some of these last catalysts, already showing an appreciable activity below 350°C, are promising substances for catalytic-trap development. Particularly, the following three compositions ($Cs_4V_2O_7$, $Cs_2O \cdot V_2O_5$, and $CsVO_3$) proved to be particularly active. For this reason, they were selected for the present investigation.

Catalyst-soot contact conditions

In Figure 1 the possible contact conditions for nonmobile (such as noble metals, perovskites, or $CsVO_3$) and mobile (such as $Cs_2O \cdot V_2O_5$) catalysts are sketched. As reported in Figure 1a, in the case of a nonmobile catalyst, the catalytic effect is limited to a few contact points between soot and solid catalyst. Conversely, it is shown that three different mobility mechanisms and two kinds of indirect catalysis may exist.

Catalysts forming volatile compounds at their operating temperatures (such as a Cu–K–Mo catalyst generating volatile Mo compounds, or KI coupled with KVO_3, which releases I_2 vapors; Badini et al., 1998) work through a gas-phase transport (Figure 1b), whereas catalysts forming liquids (such as $Cs_2O \cdot V_2O_5$, one of the material tested here) enable a liquid-phase transport of their active species. The first option is not suitable for diesel engine applications. Due to the high space velocities of the exhausts, loss of catalyst is actually unavoidable. Conversely, the materials that show liquid-phase mobility, seem to have a potential of practical application, provided they are stable under working conditions (that is, they possess low volatility, high viscosity, and good filter-material wettability, so as to remain in the filter despite the drag force exerted by the flowing gases). In this case, it is also possible to distinguish a wetting or nonwetting state: as shown in Figure 1c, the catalyst, thanks to favorable surface-tension conditions and capillary forces, can move toward soot agglomerate, wetting the entire particulate surface. In a nonwetting situation (Figure 1d), the formation of eutectic liquids allows the catalyst to rapidly offer new catalytic species to diesel particulate during its combustion.

Conversely, some catalysts can oxidize soot without having intimate physical contact. They catalyze the formation of mobile oxidizing species (such as NO_2 and O_{ads}) that are more reactive than O_2. In the absence of physical contact, the formation of those mobile oxidizing species is the most advantageous property of this type of catalyst. Two main reaction mechanisms are known for indirect-contact catalysts: oxygen spillover and the NO_x-aided gas-phase mechanism. Some catalysts can dissociate oxygen and transfer it to the soot particle by spillover (van Setten et al., 2001). On the other hand, the most pronounced effect of Pt on catalytic oxidation of soot discussed so far in the literature is to facilitate NO oxidation to NO_2 (Liu et al., 2001). The NO_2 generated on Pt is transported via the gas phase over soot particles to oxidize carbon while being reduced to NO (Uchisawa et al., 1998; Ciambelli et al., 2000).

Most catalysts require direct physical contact with carbonaceous materials if oxidation is to be accelerated. There are no standard methods of testing the soot oxidation activity of a catalyst, and the type of contact applied in each specific study becomes very important. When the soot and catalyst powders are mixed with a spatula, the contact mode is *loose*, which simulates the actual contact conditions occurring in a particulate trap. When mixing is carried out in a ball mill, it is possible to achieve a *tight contact* condition, which is useful to define an intrinsic catalytic activity under optimal contact conditions. Some catalysts showed a high or moderate activity in tight- as well as in loose-contact mode, while others were found to be active in tight-contact mode and showed no significant activity in loose-contact mode (van Setten et al., 2001). The intrinsic catalytic activity is not only necessary to obtain high carbon conversion rates, but mobility of the catalytic species is an important requisite for applications in diesel-exhaust treatment. It is clear that the performance of a

catalyst mixed with soot in tight mode cannot reproduce the tests of a real diesel engine and the contact conditions that take place in a trap. On the other hand, it is necessary to perform kinetic and mechanism studies in tight contact so as to establish good reproducibility of the experiments and determine intrinsic kinetic parameters.

Experimental Studies

Catalyst preparation

Three catalysts were synthesized from cesium carbonate and vanadium pentoxide stoichiometric mixtures. After drying at 200°C in air, the following reactions were promoted between the precursors

$$2Cs_2CO_3 + V_2O_5 \rightarrow Cs_4V_2O_7 + 2CO_2$$
$$Cs_2CO_3 + V_2O_5 \rightarrow Cs_2O \cdot V_2O_5 + CO_2$$
$$Cs_2CO_3 + V_2O_5 \rightarrow 2CsVO_3 + CO_2$$

by raising the temperature to their melting points ($Cs_4V_2O_7$: 870°C; $Cs_2O \cdot V_2O_5$: 380°C; $CsVO_3$: 641°C; Roth et al., 1969) in a ceramic crucible under an air atmosphere. After a 2 h stay at a high temperature, the cesium pyrovanadate and metavanadate were annealed for 24 h in air at 300°C, while the oxide mixture was annealed at 250°C, because of its low melting point (380°C). All the catalysts were then ground in a ball mill at room temperature. The compositions of the powders obtained were checked by X-ray diffraction (PW1710 Philips diffractometer; Cu-K_α radiation), which confirmed the success of the preparation route. SEM observation (Philips 515 SEM) allowed to assess that the average grain size of the catalysts prepared was in the 10–20-μm range.

Carbonaceous materials

An amorphous carbon (average particle size: 45 nm; 0.34% ashes after calcination at 800°C; 12.2 wt % of moisture lost after drying at 110°C) was used, instead of real diesel soot, in order to compare the activity toward CO_2 of different catalysts and to assess the prevalent kinetic parameters of all catalysts. Different commercial carbon blacks produced by Cabot Ltd. were used (see Table 2) for the evaluation of the preexponential factor and the effect of the particle size on the combustion rate.

These materials were preferred over their real counterparts so as to avoid any interfering effect due to the presence of adsorbed hydrocarbons, sulfates, or fly ashes present in real diesel soot. Furthermore, the amorphous and the commercial carbon employed are more difficult to burn than real diesel soot, which renders the achieved activity results conservative (for more details, see Figure 2; Serra et al., 1997).

Differential scanning calorimetry (DSC)

The activation energy E_a was measured via differential scanning calorimetry (DSC) (Perkin Elmer DSC-Pyris) and the so-called Ozawa method (Ozawa, 1970, 1975). DSC experiments were performed on mixtures of catalysts with carbon (obtained by careful grinding in an agate mortar) so as to measure the heat released as an index of the evolution of catalytic combustion. Under an air flow of 100 $mL \cdot min^{-1}$, a mixture of catalyst and carbon (2:1 mass basis) was placed in the sample crucible, whereas an equal weight of alumina was used as a reference. Temperature was increased from 50°C to 700°C, with different heating rates ($\phi = 5$, 10, 20, 30, and 50°C/min). Several plots representing exothermal combustion peaks were obtained. These patterns were processed to point out the temperature corresponding to the cumulative combustion of 25, 50, and 75 wt % of the total initial carbon located in the sample holder. Some tests were also performed on an alumina/carbon mixture to evaluate the activation energy of the noncatalyzed carbon combustion.

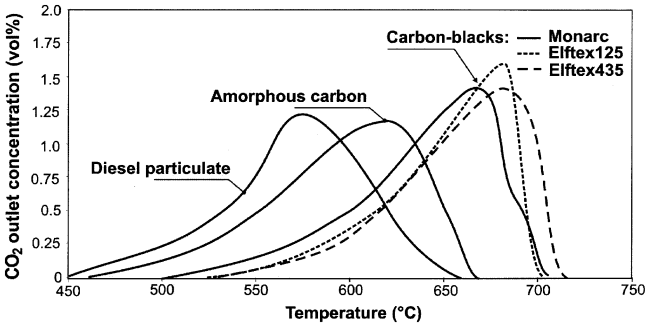

Figure 2. Noncatalytic TPC runs performed with several commercial carbons and with a real diesel particulate.

Isothermal and temperature-programmed combustion

Isothermal combustion (ITC) tests were then carried out to evaluate k_∞ and β (see Eq. 1 at the beginning of the section on activation energy), using catalyst/carbon/SiO_2 2:1:15 (mass basis) mixtures located inside a microreactor between two layers of quartz wool (0.25–0.4-mm silica grains were used to prevent thermal runaways and reduce the pressure drop). The reactor was heated via an electric oven with a PID temperature regulation system. The temperature was raised to a constant operating value (in the range 300–450°C) under helium flow. The reacting gas (characterized by different O_2 concentrations in He: for example, 5, 2.5, and 1 vol %) was then fed to the microreactor at the constant rate of 50 mL/min. The CO_2 concentration in the outlet gas flow was analyzed by a CO_2 NDIR analyzer.

Screening tests were also performed in a temperature-programmed-combustion (TPC) apparatus in order to determine some critical performance parameters of each of the prepared catalysts (such as catalyst activity, selectivity to CO_2 of carbon conversion, optimal operating temperature range, and so on). Air was fed to a fixed-bed microreactor constituted of a 1:2:15 by weight mixture of carbon, powdered catalyst, and SiO_2 granules at the constant rate of 50 mL/min. The reactor temperature was controlled through a PID-regulated oven and varied during each TPO run from 200°C to 700°C at a $5°C \cdot min^{-1}$ rate, after being at 200°C under He flow for 15 min as a common pretreatment. The analysis of the outlet reactor gas was performed through a CO_2 NDIR analyzer. Some comparative TPC runs were also performed in the absence of the catalysts (noncatalytic combustion) with all the different carbonaceous materials considered in the present investigation.

Heated optical microscope

Wettability studies between the $Cs_2O \cdot V_2O_5$ catalyst and carbon were carried out by preparing a tablet of amorphous carbon, above which a small agglomerate of catalyst powders was placed, and by locating it inside the oven of the heating microscope at room temperature. The temperature was increased up to melting point and beyond with a heating rate of $5°C \cdot min^{-1}$, meanwhile monitoring the contact angle between catalyst and carbon by direct observation.

Theory

Activation energy

A kinetic law for diesel particulate catalytic combustion should account for several parameters. Previous investigations (Ciambelli et al., 1996) showed that an Arrhenius-type expression, including power-law dependence on the oxygen partial pressure, holds for most diesel combustion catalysts

$$r = k_\infty \exp\left(-\frac{E_a}{RT}\right) p_{O_2}^{\beta} \tag{1}$$

The activation energy can be evaluated through the so-called Ozawa procedure (Ozawa, 1970), an updated version of the Kissinger method (Kissinger, 1957), by proper interpretation of thermal analysis data (DSC in the present investigation). According to this procedure, the following correlation associates the values of the heating rate Φ and the corresponding values of temperature (T_α) at which a fixed fraction α of carbon is burned during each run

$$\ln \Phi = B - 0.4567 \cdot \left(\frac{E_a}{RT_\alpha}\right) \tag{2}$$

where B is a constant lumping α-dependent terms. If the heat released by the combustion is assumed to be proportional to the fraction α of converted carbon, once chosen, a fixed α value (such as 50%), the T_α value corresponding to such value can be easily derived from the DSC curves by evaluating, via a simple integration, the amount of heat released by combustion. By least-square fitting of the ln Φ-vs.-$1/T_\alpha$ data series, estimates of the activation energy can be derived from the slope of the best-fitting lines.

An indirect validation of the obtained E_a value can be accomplished via a proper interpretation of the start of the ITC plots. These plots are characterized by a rapid initial rise of the CO_2 outlet concentration until a maximum (c_{max}) is reached (see Figure 7). The reason why it is related to the presence of the gas volume inside the apparatus (mostly corresponding to the cell where the NIDR detector is located)

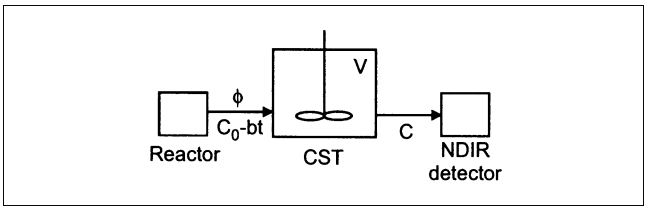

Figure 3. Representation of the volume between the TPC reactor and the NDIR detector.

where back-mixing phenomena are significant. This volume V can be schematized as an ideal continuously stirred tank, a simple model representation that accounts for the occurrence of back mixing mentioned (see Figure 3).

It can be assumed that in the early reaction phases the CO_2 outlet concentration decreases with time according to a linear law $c_0(1\text{-}bt)$ that corresponds to a first-order dependency of the reaction rate vs. the available carbon mass in contact with the catalyst, all other conditions being equal. The volumetric outlet flow rate F being constant, the following balance equation over the volume, V, can then be written

$$\frac{dc}{dt} + \frac{F}{V}c - \frac{F}{V}c_0(1 - bt) = 0 \tag{3}$$

where, since $c(0) = 0$, the solution becomes

$$c(t) = c_0\left(1 + \frac{V}{F}b\right)(1 - e^{-(F/V)t}) - bc_o t \tag{4}$$

It can be easily demonstrated that the maximum concentration of the ITC plot can thus be expressed as

$$c_{max} = c_0\left[1 - \frac{Vb}{F}\ln\left(1 + \frac{F}{Vb}\right)\right] \tag{5}$$

Based on the preceding assumptions, it can be concluded that the maximum of the ITC curves should be proportional to the initial concentration, c_0. This last concentration, in its turn, is proportional to the kinetic constant as long as the oxygen partial pressure variation throughout the reactor is negligible. If the type of contact conditions between catalyst and carbon remains the same (which is likely to occur in the early stages of the ITC run), the preexponential kinetic constant, k_∞, should remain equal for each catalyst at the different temperature values, and the c_{max} value results in a function of the activation energy. The following equation can be proposed

$$\frac{(c_{max})_1}{(c_{max})_2} = \exp\left(-\frac{E_a}{RT_1}\right) \Big/ \exp\left(-\frac{E_a}{RT_2}\right) \tag{6}$$

This expression will be employed later in the analysis of the ITC plots of the two most promising catalysts studied ($Cs_2O \cdot V_2O_5$, $Cs_4V_2O_7$) so as to confirm of the accuracy of the E_a values derived with the Ozawa method.

Other kinetic parameters

The reaction order β can be derived from ITC data obtained at different p_{O_2} values. The rate of carbon converted per unit time (r) can be calculated for each catalyst and p_{O_2} value via a simple carbon mass balance, at equal carbon-to-catalyst ratios and temperature values. Hence, β and k_∞ can be evaluated from the slope and the y-axis intercept of the least-square fitting line of logarithmic data plots.

Conversely, k_∞ is a function of the catalyst and carbon particle size as well as of the relative amount of such components in the reactants mixture. At least for the cases represented in Figures 1a and 1d, k_∞ can be set proportional to the number of contact points between the carbon and the catalyst particles. Owing to the experimental conditions

adopted in TPC and ITC runs, the following assumptions could be made:

- The carbon particles can be considered as spherical;
- The amount of carbon is enough to form a monolayer of particles on the catalyst surface (the 2:1 catalyst-to-carbon weight ratio corresponds roughly to a 1:5 volume ratio, as the counterparts have different density);
- The catalyst–carbon mixture is homogeneous and reproducible (the powders were mixed in a mortar);
- The catalyst particle size is not affected by the adopted mixing procedure (as confirmed by specific SEM observations of the catalyst before and after mixing);
- The catalyst surface can be considered like a flat surface from the viewpoint of the carbon particles (the size of these particles is by at least 100-fold smaller than that of the catalyst, as checked by SEM analysis; see the section on catalyst preparation).

The number of contact points should then be equal to the ratio between the available catalyst surface (a constant value in all the runs with the same catalyst) and the part of this surface occupied by a single carbon particle, proportional to the square of the diameter of this latter. Hence, if carbon particles of a different size (such as the carbon blacks considered) are adopted in the ITC tests, the following relationship should be valid: $k_\infty \propto d_C^{-2}$.

It can be easily demonstrated that, if k_∞ were proportional to the external soot agglomerate geometrical surface (a case more properly representing the condition depicted in Figure 1c), it would be a linear function of just d_C^{-1} (Serra et al., 1997). The k_∞-vs.-d_C experimental data can thus provide indications about the actual mechanism through which the catalyst promotes carbon combustion, as discussed later.

Results and Discussion

Some preliminary considerations concerning the TPC curves (Figure 2) obtained for the noncatalytic combustion of the various types of soot considered can be expressed. These data show that diesel particulate can be burned out at temperatures lower than those characteristic of the other "dry" carbons tested. This is mainly due to the presence of a soluble organic fraction (33 wt % in the diesel particulate adopted in the experiment). It is likely that combustion is initiated by the polyaromatic hydrocarbons adsorbed over the carbon nuclei and then transferred by a localized heating to the solid carbon nuclei themselves. The presence of hydrocarbons could render much more complex the kinetics and reaction mechanism analysis. Therefore, amorphous carbon was used for such an investigation, as this soot is, among dry ones, the one that burns at temperatures closer to those characteristics of diesel particulate. Conversely, the three carbon blacks, selected for their different and well-defined particle size (see Table 2), do burn in a similar temperature range, a prerequisite that lends reliability to the experimental analysis of the role of d_C on the preexponential kinetic constant.

As far as the comparative analysis of the activity of the catalysts toward soot combustion is concerned, the TPC curves plotted in Figure 4 show that all catalysts significantly shift the combustion temperature range toward temperature values lower than those typical of noncatalytic combustion. The activity order in *tight-contact* conditions is $Cs_4V_2O_7 > Cs_2O \cdot V_2O_5 > CsVO_3$. The superior activity of cesium pyrovanadate, melting at 870°C, is likely to be attributed to its capability of promoting oxygen spillover (Figure 1e; Saracco et al., 1999). The high mobility of oxygen species is related to the high oxygen-to-vanadium ratio of this compound compared to its two counterparts. Furthermore, the high electropositivity of cesium ($Cs_4V_2O_7$ has the highest Cs-to-V ratio among the considered catalysts) entails an electron-donating effect that should further weaken the stability of V=O bonds (Mross, 1983).

The good catalytic activity shown by the $Cs_2O \cdot V_2O_5$ is conversely related to its capability of producing a eutectic liquid among its compounds already at 380°C (Roth et al., 1969), as confirmed by a specific DSC run performed with the catalyst alone. As mentioned earlier, a specific test was carried out in a heated optical microscope in order to better determine whether such a liquid phase was capable of wetting the soot or not (Figure 1c or 1d). Figure 5 shows the occurrence of liquid formation when 380°C are exceeded. The derived liquid cannot wet the carbon (see the picture taken at 420°C), and the area of contact between catalyst and carbon remains limited. However, it has to be emphasized that the higher the temperature, the wider the area of carbon–catalyst contact is expected to be. The type of contact conditions between the $Cs_2O \cdot V_2O_5$ eutectic liquid and carbon in a real catalytic trap

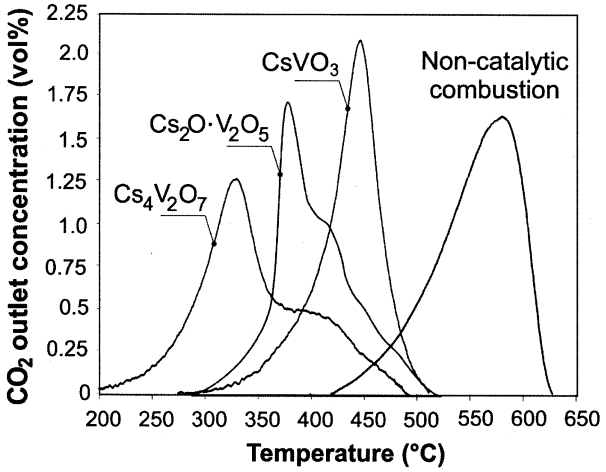

Figure 4. TPC runs performed with $Cs_4V_2O_7$, $Cs_2O \cdot V_2O_5$, and $CsVO_3$ catalysts; the noncatalytic carbon combustion is also considered for comparison.

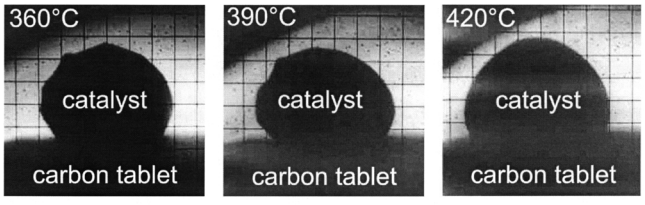

Figure 5. Pictures of a $Cs_2O \cdot V_2O_5$ catalyst sample obtained in a thermal microscope in calm air: (a) 360°C (solid catalyst); (b) 390°C (slightly above the start of eutectic liquid formation); (c) 420°C (molten catalyst).

Table 1. Prevalent Kinetics Parameters Derived for Different Catalysts by Use of Amorphous Carbon as a Particulate Source

Catalysts	k_∞ ($s^{-1} \cdot Pa^{-\beta}$)	β	E_a^* (kJ/mol)
$CsVO_3$	154.6	1.00	125
$Cs_4V_2O_7$	4,087	0.68	104
$Cs_2O \cdot V_2O_5$	3,811	0.79	123

* Noncatalytic diesel-soot combustion: 157 kJ/mol.

should be those depicted in Figure 1d. Conversely, the melting temperature of the less-active $CsVO_3$ (641°C; Saracco et al., 1999) is too high to let liquid formation affect the evolution of carbon combustion, which thus should be governed by the mechanisms depicted in Figures 1a and, possibly, 1e.

Turning to the analysis of kinetic data, we find the values of the kinetic parameters determined for the combustion of amorphous carbon listed in Table 1.

The activation energy obtained for all the catalysts is much lower than that of noncatalytic combustion. The $Cs_4V_2O_7$ has a rather low E_a value (104 kJ/mol), about two-thirds of that of the noncatalytic combustion, which is in line with its prevalent activity (Figure 4). The activation energy of the $Cs_2O \cdot V_2O_5$ is almost equal to that of the $CsVO_3$ one, which indicates that the type of oxygen species delivered by these two catalysts to the combustion process should be similar. This, of course, cannot explain the difference in activity between these two catalysts (see Figure 4). The formation of eutectic liquids should be a key player in this context. By analyzing the DSC plots obtained at different temperature-increase rates for the assessment of E_a for the $Cs_2O \cdot V_2O_5$ catalyst, a sudden slope variation can be noticed in the DSC curves at temperatures close to 400°C, especially at low temperature-rise rates (Figure 6). This occurrence is related to the formation of the previously mentioned eutectic liquid that speeds up the combustion process by enabling catalyst mobility and better contact conditions between carbon and catalytically active species. If the Ozawa plots obtained for the $Cs_2O \cdot V_2O_5$ catalyst at different carbon conversions (α) are considered (Figure 7), it can be seen clearly that no appreciable change in the slope of the data points occurs for higher temperatures than the one related to the formation of the first amounts of eutectic liquid. This means that the activation energy of the combustion process is not markedly influenced by the formation of liquid. Hence, the higher conversion rates achievable with the $Cs_2O \cdot V_2O_5$ catalyst against the $CsVO_3$ one mainly should be due to the increase of the preexponential kinetic constant. This parameter accounts for the number of useful contacts between carbon and active oxidizing species achieved per unit time. The preceding argument is perfectly in line with the values of the k_∞ measured for the three catalysts (Table 1). The preexponential constant of the $Cs_2O \cdot V_2O_5$ catalyst is one order of magnitude higher than those of $CsVO_3$, which is due to the mobility of its active components. Conversely, $Cs_4V_2O_7$ shows a k_∞ value of the same order of magnitude as the $Cs_2O \cdot V_2O_5$ catalyst, which should be directly related to its capability of inducing oxygen spillover.

Further examples of these merits can be found in the ITC plots of Figure 8 obtained for the two most active catalysts ($Cs_4V_2O_7$ and $Cs_2O \cdot V_2O_5$) at different operating temperatures. The start of the ITC process is qualitatively similar for

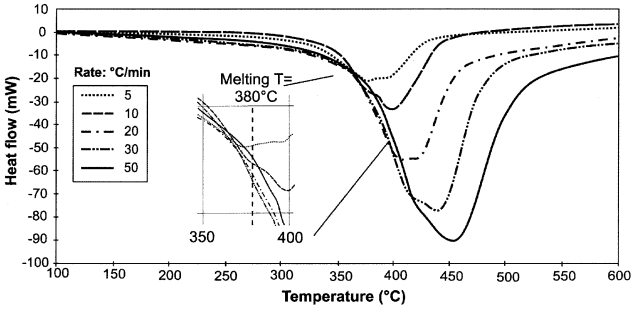

Figure 6. DSC plots for catalytic combustion of amorphous carbon over the $Cs_2O \cdot V_2O_5$ catalyst at different heating rates.

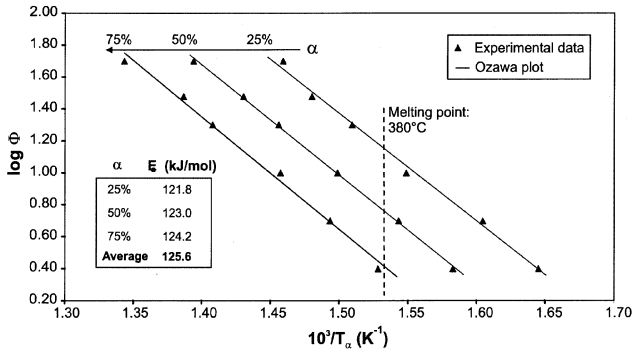

Figure 7. Ozawa plots of the $Cs_2O \cdot V_2O_5$ catalyst for the determination of the activation energy (E_a) at different levels of carbon conversion (α).

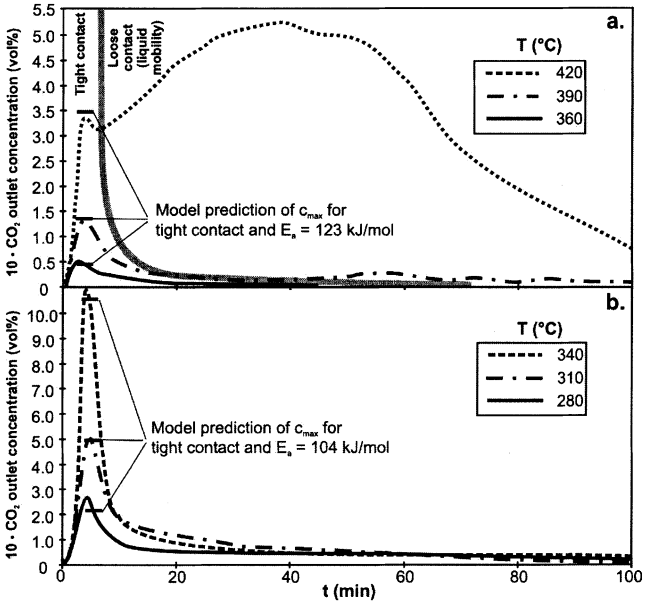

Figure 8. ITC curves obtained for (a) the $Cs_2O \cdot V_2O_5$ and (b) the $Cs_4V_2O_7$ catalysts at different operating temperatures with a 2.5 vol % concentration of O_2 in the feed.

the two catalysts, leading to a bell-shaped curve. The maximum values of the outlet CO_2 concentration curves obtained at different temperatures for each single catalyst can be related to one another through Eq. 9. The best-fit estimates of these values are provided in Figure 8 by using the activation energy values determined via the Ozawa method (Table 1). The good agreement between model estimates and experimental data obtained provides an indirect validation of the Ozawa method itself and adds reliability to the E_a values evaluated by these means.

A significant difference can be noticed, however, in the shape of the ITC curves of the two considered catalysts after the maximum has been reached. The curves obtained for the $Cs_4V_2O_7$ catalyst (Figure 8b) show an asymptotic trend toward zero CO_2 production along with the progressive combustion of the entire carbon mass. Conversely, for the $Cs_2O \cdot V_2O_5$ (Figure 8a) this trend is followed just by the curve recorded at the lowest temperature (360°C). For temperatures higher than the liquid-formation one (380°C), after the bell-shaped region, the curves become more irregular, showing at least one further maximum value. This is particularly evident for the curve related to 420°C, where the eutectic liquid has become less viscous than at 390°C. This behavior might be explained by the two following points:

(1) At the beginning of the ITC runs, good contact conditions between catalyst and carbon were allowed by the catalyst–carbon mixing method adopted (*tight contact*), and the significant carbon fraction in direct contact with the catalyst burns out at first entering the bell-shaped region of the curve;

(2) The remaining fraction of carbon is then reached by the liquid phase generated by the catalyst under *loose-contact* conditions. This is a typical behavior of carbon gasification catalysts (Mross, 1985).

This provides the $Cs_2O \cdot V_2O_5$ catalyst with a good chance of success in practical catalytic-trap applications where the contact conditions between catalyst and carbon are not as tight as they were forced, for reproducibility reasons, in the microreactor runs performed in the present investigation (van Setten et al., 2001).

The activity of the $Cs_4V_2O_7$ catalyst is even higher than that of the $Cs_2O \cdot V_2O_5$ catalyst, since it seems to enable the spillover of quite active oxygen species. However, a weak point of this catalyst is its high solubility in water, which limits its applicability to stationary, large-scale applications. In mobile applications, the frequent shutdowns of the diesel engines would, in fact, promote water condensation in the exhaust line and in the trap itself, with consequent catalyst dissolution.

The results of the ITC runs carried out with carbon blacks with different diameters, listed in Table 2, confirm the order-of-magnitude difference between the k_∞ values measured for the $Cs_2O \cdot V_2O_5$ and $Cs_4V_2O_7$ catalysts compared with those of the other ones. Furthermore, they show that the preexponential kinetic factor is, in fact, influenced by d_C, and particularly increases when the carbon particle diameter is decreased. More precisely, Figure 9 shows that for any of the catalyst k_∞ that is proportional to the inverse of d_C^2. According to the theoretical arguments proposed in the section on activation energy, this should be so for those catalysts that are solid ($Cs_4V_2O_7$ and $CsVO_3$) or at least do not wet the carbon particles ($Cs_2O \cdot V_2O_5$).

Table 2. Basic Properties of Carbon Blacks* and Values of the k_∞ Constant as a Function of the Particulate Size

Trade Name	Avg. Particle Size (nm)	BET Area ($m^2 \cdot g^{-1}$)	k_∞ ($s^{-1} \cdot Pa^{-\beta}$)		
			$CsVO_3$	$Cs_4V_2O_7$	$Cs_2O \cdot V_2O_5$
Monarc 700	18	200	25.2	163.7	161.6
Elftex 435	27	80	23.7	89.5	148.5
Elftex 125	60	30	22.0	65.3	142.3

*Carbon blacks courtesy of Cabot Ltd.

Some final considerations must be addressed to the reaction orders of oxygen listed in Table 1. The fractional β values of the $Cs_4V_2O_7$ and $Cs_2O \cdot V_2O_5$ catalysts suggest that oxygen chemisorption from the atmosphere should occur according to the Langmuir-type mechanism (Satterfield, 1991), which confirms that these catalysts likely act as an oxygen pump toward carbon. Conversely, oxygen chemisorption over $CsVO_3$ at the catalyst operating temperatures should be weaker and/or not at equilibrium, as its reaction order is 1.

Conclusions

A thorough experimental and modeling analysis has been carried out for three of the most promising catalysts ($Cs_2O \cdot V_2O_5$, $Cs_4V_2O_7$, CVO_3) for application in catalytic traps for diesel particulate removal in order to better assess the soot combustion process they promote.

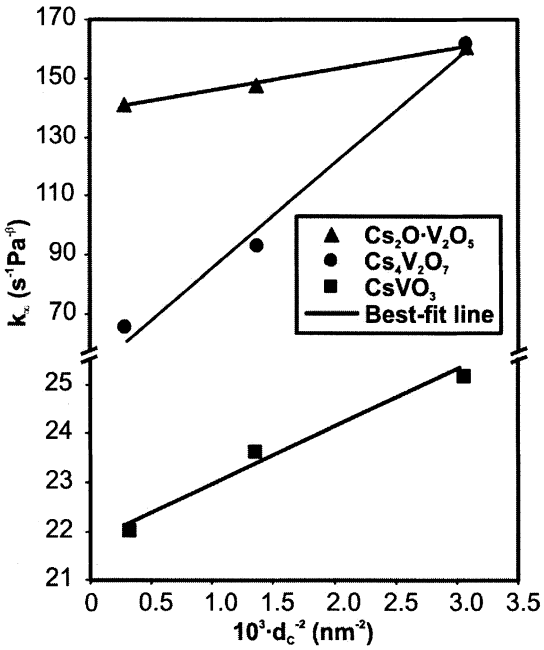

Figure 9. Effect of particle size of carbon blacks on the preexponential kinetic constant of the $Cs_4V_2O_7$, $Cs_2O \cdot V_2O_5$, and the $CsVO_3$ catalysts.

It has been shown that beyond the intrinsic activity of the catalytic species (excellent for the $Cs_4V_2O_7$ catalyst), their mobility, achieved by the $Cs_2O \cdot V_2O_5$ via eutectic liquid formation and by $Cs_4V_2O_7$ via oxygen spillover, is a quite important requisite for practical application in diesel particulate traps. Nevertheless, the application of mobile catalysts for the after-treatment of diesel exhausts requires a careful evaluation of their stability. The severe operating conditions characteristic of the exhaust line of diesel engines (temperature peaks, high space velocities, and so on) might lead to loss of active compounds by drag or by evaporation. Some encouraging preliminary tests on catalytic foam traps using $Cs_2O \cdot V_2O_5$ show only a limited catalyst deactivation of this catalyst after prolonged use.

Finally, the reader must be warned that the derived intrinsic kinetic expressions, useful to express some features concerning the role of mobile species on the catalytic activity, cannot be directly used in numerical models for the design optimization of catalytic traps. Several exhaust-gas components (water, NO_x, SO_x, hydrocarbons, to name four), not considered here, may have a significant effect on the catalyst activity and stability (for example, Serra et al., 1996; Fino et al., 2002). Furthermore, as stated earlier, the catalyst–soot contact conditions in these multifunctional reactors are typically loose (van Setten et al., 2001) and not tight as in most of the experiments carried out in the present investigation.

Acknowledgments

Financial support of the European Community (projects CATATRAP, ART-DEXA, and SYLOC-DEXA) is gratefully acknowledged.

Notation

b = decay constant
B = constant in the Ozawa method
c = CO_2 concentration at the NDIR detector, vol %
c_0 = CO_2 concentration at the reactor outlet in a ITC run, vol %
d_C = soot particle diameter, m
E_a = activation energy, $kJ \cdot mol^{-1}$
F = volumetric flow rate, $N \cdot m^3 \cdot s^{-1}$
$f(\alpha)$ = whatever function of α
k' = kinetic constant in the Ozawa theory, s^{-1}
k'_∞ = preexponential kinetic constant in the Ozawa theory, s^{-1}
k_∞ = preexponential constant, $Pa^{-\beta} \cdot s^{-1}$
p_{O_2} = oxygen partial pressure, Pa
r = soot reaction rate per unit catalyst mass, s^{-1}
R = ideal gas constant = 8.314 J/mol/K
t = time, s
T = absolute temperature, K
T_α = temperature at which a given α value is reached, K
V = model continuously stirred volume, m^3

Greek letters

α = fraction of converted soot
β = oxygen reaction order
Φ = heating rate, $K \cdot s^{-1}$
ζ_{CO_2} = selectivity toward CO_2

Literature Cited

Ahlstrom, A. F., and C. U. I. Odenbrand, "Combustion of Soot Deposits from Diesel Engines on Mixed Oxides of Vanadium Pentoxide and Cupric Oxide," *Appl. Catal.*, **60**, 157 (1990).

Badini, C., G. Saracco, and V. Specchia, "Combustion of Carbon Particulate Catalyzed by Mixed Potassium Vanadates and KI," *Catal. Lett.*, **55**, 201 (1998).

Badini, C., G. Saracco, N. Russo, and V. Specchia, "A Screening Study on the Activation Energy of Vanadate Based Catalysts for Diesel Soot Combustion," *Catal. Lett.*, **69**(3/4), 207 (2000).

Ciambelli, P., P. Corbo, M. Gambino, V. Palma, and S. Vaccaro, "Catalytic Combustion of Carbon Particulate," *Catal. Today*, **27**, 99 (1996).

Ciambelli, P., V. Palma, P. Russo, and S. Vaccaro, "The Role of NO in the Regeneration of Catalytic Ceramic Filters for Soot Removal from Exhaust Gases," *Catal. Today*, **60**, 43 (2000).

Fino, D., G. Saracco, and V. Specchia, "Filtration and Catalytic Abatement of Diesel Particulate from Stationary Sources," *Chem. Eng. Sci.*, **57**, 4955 (2002).

Kissinger, H. E., "Reaction Kinetics in Differential Thermal Analysis," *Anal. Chem.*, **29**, 1702 (1957).

Konstandopoulos, A. G., M. Kostoglou, E. Skaperdas, E. Papaioannou, D. Zarvalis, and E. Kladopoulou, "Fundamental Studies of Diesel Particulate Filters: Transient Loading, Regeneration and Aging," *Diesel Aftertreatment 2000*, Vol. SP-1497, Society of Automotive Engineers, ed., Detroit, MI, p. 189 (2000).

Liu, S., A. Obuchi, O.-J. Uchisawa, T. Nanba, and S. Kushiyama, "Synergistic Catalysis of Carbon Black Oxidation by Pt with MoO_3 or V_2O_5," *Appl. Catal. B: Environ.*, **30**, 259 (2001).

Mariangeli, R. E., E. H. Homier, and F. S. Molinaro, *Catalysis and Automotive Pollution Control*, Elsevier, Amsterdam, p. 457 (1987).

McKee, D. W., and D. Chatterji, "Catalytic Behaviour of Alkali Metal Salts in Graphite Gasification Reactions," *Carbon*, **13**, 381 (1975).

Mross, W. D., "Alkali Doping in Heterogeneous Catalysis," *Catal. Rev.—Sci. Eng.*, **25**, 591 (1983).

Mul, G., J. P. A. Neeft, F. Kapteijn, M. Makkee, and J. A. Moulijn, "Soot Oxidation Catalysed by a Cu/K/Mo/Cl Catalyst: Evaluation of the Chemistry and Performance of the Catalyst," *Appl. Catal. B: Environ.*, **6**, 339 (1995).

Neeft, J. P. A., M. Makkee, and J. A. Moulijn, "Catalysts for the Oxidation of Soot from Diesel Exhaust Gases. I. An Exploratory Study," *Appl. Catal. B: Environ.*, **8**, 57 (1996).

Ozawa, T., "Kinetic Analysis of Derivate Curves in Thermal Analysis," *J. Thermal Anal.*, **2**, 301 (1970).

Ozawa, T., "Critical Investigation of Methods for Kinetic Analysis of Thermo-Analytical Data," *J. Thermal Anal.*, **7**, 601 (1975).

Roth, R. S., T. Negas, and L. P. Cook, *Phase Diagrams for Ceramists*, Compiled at the National Bureau of Standards, American Chemical Society, Washington, DC (1969).

Saracco, G., C. Badini, N. Russo, and V. Specchia, "Development of Catalysts Based on Pyrovanadates for Diesel Soot Combustion," *Appl. Catal. B: Environ.*, **21**, 233 (1999).

Saracco, G., V. Serra, C. Badini, and V. Specchia, "Potential of Mixed Halides and Vanadates as Catalysts for Soot Combustion," *Ind. Eng. Chem. Res.*, **36**, 2051 (1997).

Satterfield, C. N., *Heterogeneous Catalysis in Industrial Practice*, McGraw-Hill, New York (1991).

Serra, V., G. Saracco, C. Badini, and V. Specchia, "Cu-K-V Catalysts for Diesel Soot Combustion," *Riv. Combust.*, **50**, 383 (1996).

Serra, V., G. Saracco, C. Badini, and V. Specchia, "Combustion of Carbonaceous Materials by Cu-K-V Based Catalysts: II. Reaction Mechanism," *Appl. Catal. B: Environ.*, **11**, 329 (1997).

Uchisawa, J.-O., A. Obuchi, Z. Zhao, and S. Kushiyama. "Carbon Oxidation with Platinum Supported Catalyst," *Appl. Catal. B: Environ.*, **18**, L183 (1998).

van Setten, B. A. A. L., M. Makkee, and J. A. Moulijn, "Science and Technology of Catalytic Diesel Particulate Filters," *Catal. Rev. Sci. Eng.*, **43**, 489 (2001).

Watabe, Y., K. Yrako, T. Miyajimo, T. Yoshimoto, and Y. Murakami, "'Trapless' Trap—A Catalytic Combustion System of Diesel Particulates Using Ceramic Foam," SAE paper Nr. 830082, Society of Automotive Engineers, Detroit, MI (1983).

Manuscript received Oct. 28, 2002, and revision received Feb. 19, 2003.